Electronic origin of the isostructural decomposition in cubic $M_{1-x}Al_xN$ (M=Ti, Cr, Sc, Hf): A first-principles study

Björn Alling, A Karimi and Igor Abrikosov

Original Publication:

Björn Alling, A Karimi and Igor Abrikosov, Electronic origin of the isostructural decomposition in cubic $M_{1-x}Al_xN$ (M=Ti, Cr, Sc, Hf): A first-principles study, 2008, Surface and Coatings Technology, (203), 5-7, 883-886.
http://dx.doi.org/10.1016/j.surfcoat.2008.08.027

Electronic Origin of the Isostructural Decomposition in cubic $M_{1-x}Al_xN$ (M=Ti, Cr, Sc, Hf): a first-principles study

B. Alling,[1,2,*] A. Karimi,[1] and I. A. Abrikosov[2]

[1] *Institute of Physics of Complex Matter, Swiss Federal Institute of Technology Lausanne (EPFL), 1015 Lausanne, Switzerland*
[2] *Department of Physics, Chemistry and Biology (IFM), Linköping University, SE-581 83 Linköping, Sweden*

(Dated: November 3, 2009)

We have used first-principles calculations to investigate the mixing enthalpies, lattice parameters and electronic density of states of the ternary nitride systems $Ti_{1-x}Al_xN$, $Cr_{1-x}Al_xN$, $Sc_{1-x}Al_xN$ and $Hf_{1-x}Al_xN$ in the cubic B1 structure where the transition metals and aluminium form a solid solution on the metal sublattice. We discuss the electronic origins of the possible isostructural decomposition in these materials relevant for hard coatings applications. We find that in the systems $Ti_{1-x}Al_xN$ and $Hf_{1-x}Al_xN$ the electronic structure effects strongly influences the phase stability as d-states are localised at the Fermi level in AlN-rich samples. This leads to a strongly asymmetric contribution to the mixing enthalpy, an effect not present in $Cr_{1-x}Al_xN$ and $Sc_{1-x}Al_xN$. The lattice mismatch is large in $Sc_{1-x}Al_xN$ and $Hf_{1-x}Al_xN$, giving a symmetric contribution to the mixing enthalpies in those systems.

PACS numbers:

INTRODUCTION

To increase the hardness and prolong the lifetime of cutting tools, coating with transition metal nitrides has been standard procedure within the industry for several decades. Today, complex multicomponent nitrides have, to a large extent, replaced the binary nitrides such as TiN. It has been found that the alloying of TiN with AlN increases the cutting performance of the coating. This has been attributed to increased oxidation resistance, but more recently also to an age-hardening mechanism [1]. This mechanism has been explained by an isostructural decomposition of cubic B1 $Ti_{1-x}Al_xN$ solid solution into coherent cubic domains of c-AlN and Ti-rich $Ti_{1-x}Al_xN$ [2]. The driving force of this decomposition was later shown, by means of first-principles calculations, to be mainly an electronic band structure effect in samples rich in AlN [3]. A related coating material, $Cr_{1-x}Al_xN$ has also been very successful in cutting tools applications. The decomposition pattern in this material is rather different compared to $Ti_{1-x}Al_xN$, lacking the isostructural decomposition [4–7] . It was shown [8] that the magnetic splitting of the Cr 3d-state was the reason for this difference. In this work we present an extension of the previous studies done on the $Ti_{1-x}Al_xN$ and $Cr_{1-x}Al_xN$ systems by including in a common comparison also $Sc_{1-x}Al_xN$ and $Hf_{1-x}Al_xN$ systems. The $Hf_{1-x}Al_xN$ system has recently been studied experimentally [9], but there is, to the best of our knowledge, yet no reports of experimental or theoretical studies of the $Sc_{1-x}Al_xN$ system although one stable Sc-Al-N phase has recently been found, the Sc_3AlN perovskite [10]. This inclusion adds an extra dimension to the study of the mixing termodynamics since ScN and HfN, in opposite to TiN and particularly CrN, show a large lattice missmatch with c-AlN. Thus we are able to analyse the contribution of both the band structure effect and volume mismatch to the atomic level drivingforce for isostructural decomposition in $M_{1-x}Al_xN$-systems.

CALCULATIONAL METHODS

The present study is performed within a density functional theory (DFT) framework. Before going into the details of the specific methods used to solve the Kohn-Sham equations, we would like to briefly discuss how one can model the distribution of the transition metal and aluminium atoms on the metal sublattice of our systems. The PVD experimental techniques used to grow the thin film materials considered here all operate at rather low substrate temperatures which limits diffusion, at least within the bulk. At the same time the surface layers are subject to a rather stochastic impact of energetic ions, a combination which are likely to hinder the system from getting even close to thermodynamical equilibrium during growth. Thus as-deposited samples of the systems considered here, within the concentration range where they are possible to grow as single phases, are likely to be very close to the high-entropy solid solution. This means that any first-principles calculation aiming at describing the physics of these systems should tackle the problem on how to calculate the electronic structure of such a random occupation of the metal sublattice.

Substitutionally disordered systems are characterised by the fact that the chemical environment of each metal atom are different. In opposite to ordered compounds there exists both transition metal atoms that have a large amount of other transition metal atoms in its direct environments at the same time as there exist transition metal

atoms that are to a very large extent surrounded by aluminium. This means that in principle the unit cell of the system is infinitely large, making it impossible to carry out conventional band structure calculations. However, within the alloy theory different methods have been developed that are capable to accurately describe solid solutions. If one wants to directly model a solid solution within a supercell framework, the accurate method is to use the so called Special Quasi-random Structure (SQS) method originally suggested by Zunger et al. [11] and extended and described in details in Ref. [3]. Within this technique one designs specific supercells in order to buy "randomness" within the first couple of nearest neighbour shells by paying the cost of a very "non-random" distribution at the more distant neighbouring shells thus using the fact that chemical interactions in crystalline solid systems in most cases are rather short ranged. In this work the supercells created in Ref.[3] has been used to calculate the mixing enthalpies and lattice parameters of the $Ti_{1-x}Al_xN$, $Sc_{1-x}Al_xN$ and $Hf_{1-x}Al_xN$ systems with concentration steps of Δx=0.125. Although it is possible to rather accurately describe the mixing enthalpy of a random system also using a careful expansion of the configurational space in a large series of different ordered structures [12], a least square fit of the energy of a couple of ad-hoc chosen supercells are likely to give values quite far from the ones obtained by state-of-the-art methods. An even more inappropriate approach would be to use the enthalpies of small ordered structures like the ones based on the $L1_0$ and $L1_2$ structures as an approximation to that of the disordered phase. Besides that the ordered and disordered phases are very different from a thermodynamics point of view, it is well known that ordered structures, for instance in the CuAu system, often show very different properties in terms of hardness and elasticity, compared to the disordered system with the same concentration.

Fig. 1 shows the calculated isostructural mixing enthalpy of B1 $Ti_{1-x}Al_xN$ using an accurate SQS method compared to the values of the $L1_0$ and $L1_2$ ordered structures and the results in Ref. [13] where a third order polynomial fit is made to the energies of some rather large but ad-hoc chosen supercells. One can see that the differences between the methods are substantial.

An alternative way to model the solid solution is to use the Coherent Potential Approximation [14–16]. In this method the physics of the random distribution is treated using a self-consistent analytical averaging of the Green's functions of the components. It was shown in Ref. [3] that in the system $Ti_{1-x}Al_xN$, the CPA method gives results in excellent agreement with the supercell approach, given that the effect of local lattice relaxations are included through a complementary model, the so-called independent sublattice model (ISM) [3]. One advantage with the CPA approach is that a paramagnetic system, such as $Cr_{1-x}Al_xN$ that is believed to have randomly oriented local magnetic moments at room temperature, can be treated as well. In this work the CPA is used to model the $Cr_{1-x}Al_xN$ system as well as to calculate the electronic density of states (DOS) of all four systems.

All our supercell calculations, as well as the calculations needed for the ISM parameters, have been made using the projector augmented wave method [17] as implemented in the Vienna *ab initio* simulation package (VASP) [18, 19]. The CPA calculations for the paramagnetic $Cr_{1-x}Al_xN$ system as well as for the electronic density of states have been performed using a Green's function technique [20–22] within the Koringa-Kohn-Rostocker [23, 24] framework and the atomic sphere approximation [25, 26]. In all calculations the Generalized Gradient Approximation [27] (GGA) has been used for the exchange-correlational energy functional. In the supercell calculations all internal atomic positions have been relaxed. All energies are converged to at least 2 meV per formula unit (f.u.) with respect to the k-point sampling of the Brillouin zone. The nitrogen sublattice is considered to be fully stoichiometric, nitrogen off-stoichiometry being treated elsewhere [28].

RESULTS

Lattice parameters

The calculated lattice parameters of our four nitride systems are shown in Fig. 2 as a function of the AlN content. The lattice parameters for the binary nitrides, TiN (4.255 Å), CrN (4.206 Å), ScN (4.521 Å), HfN (4.535 Å) and c-AlN (4.068 Å PAW and 4.094 Å KKR-ASA), are all in good agreement with the experimental ones, showing just a slight overestimation which is common for calculations using GGA functionals. The two method used in this work, the PAW and KKR-ASA methods, show a good agreement for the lattice parameter of c-AlN. This observation together with the excellent agreement between a SQS and CPA approach found in Ref. [3] justifies a direct comparison of the results obtained by means of the two methods. In the case of $Ti_{1-x}Al_xN$ and $Cr_{1-x}Al_xN$ it has previously been shown [3, 8] that first-principles calculations give results in good agreement with experimentally observed values also for the mixed systems. If we compare our results for the $Hf_{1-x}Al_xN$ system with the recent experimental results of Howe et al. [9] shown with filled triangles in Fig. 2 one can see that even though the calculated values show a positive deviation from Vegards law, it is not as large as the experimentaly observed one. One part of the explanation might be the overstoichiometry of nitrogen reported in the experiment, but not considered here. Another possible explanation might be that the experimental samples with high global AlN content might have

a certain amount of AlN in secondary phases difficult to resolve with x-ray. Thus the main B1 structure, for which the lattice parameters are measured, might have lower AlN content compared to the global content. In the case of $Sc_{1-x}Al_xN$, where no comparison with experiment is possible, there is a slight positive deviation from Vegards law.

Mixing enthalpies

The mixing enthalpy of the solid solution alone does not give all information needed for understanding the process of isostructural decomposition. However, it can be used as a starting point for deriving a mean-field approximation to the phase diagram [3] and, more importantly, unveils the basic energetics that underlies the chemical driving force for decomposition. Thus it's accurate derivation is crucial.

Fig. 3 shows the isostructural mixing enthalpies calculated as

$$\Delta H(x) = E(M_{1-x}Al_xN) - (1-x)E(MN) - xE(c-AlN) \quad (1)$$

as a function of the AlN content in each system. The energies are taken for the calculated equilibrium volume for each specific system and composition, thus setting the pressure-volume term of the enthalpies to zero. The calculated points are marked with symbols, the lines being guides for the eye. All systems show positive mixing enthalpies but the curves are still both quantitatively and qualitatively different. $Hf_{1-x}Al_xN$ has the largest values indicating the fundamental difficulty to mix HfN and AlN. The curve is strongly asymmetric with respect to equi-atomic concentrations of Hf and Al reaching its highest value close to the x=0.625 point where H=0.400 eV/f.u. $Ti_{1-x}Al_xN$ and $Sc_{1-x}Al_xN$ shows similar values of the enthalpy with a calculated maximum of ΔH=0.218 eV/f.u. in the case of $Ti_{1-x}Al_xN$ and ΔH=0.237 eV/f.u. in $Sc_{1-x}Al_xN$. However, the $Ti_{1-x}Al_xN$ curve is asymmetric in the same manner as $Hf_{1-x}Al_xN$ while the $Sc_{1-x}Al_xN$ curve is almost symmetric. The $Cr_{1-x}Al_xN$ system shows the lowest mixing enthalpy of all the systems considered here. The curve is fairly symmetric with a maximal calculated value of the enthalpy ΔH=0.074 eV/f.u.

Knowing the differences of the latticeparameters between c-AlN and the different transition metal nitrides some of the aspects of the mixing enthalpies can be understood. $Hf_{1-x}Al_xN$, with the largest mismatch has also the largest mixing enthalpy while the $Cr_{1-x}Al_xN$ has a very small mismatch and also a mixing enthalpy which is low in the present comparison. However, it is obvious that lattice mismatch can not explain all features of the mixing enthalpies. For instance, TiN has less than half the lattice mismatch to c-AlN compared to ScN and still the maximum values of their mixing enthalpies are almost equal. The volume mismatch is also unlikely to generate the asymmetric shape of the $Hf_{1-x}Al_xN$ and $Ti_{1-x}Al_xN$ curves. Instead we turn to the electronic band structure of the materials for an explanation.

Electronic density of states

The presence of an electronic band structure mismatch, rather than differences in lattice spacing, as a driving force for decomposition was discussed already in Ref. 3 for the system $Ti_{1-x}Al_xN$. It was shown that the introduction of Al in TiN gives rise to a development where the Ti 3d non-bonding state forms a sharp, atomic like, state at the Fermi level. This unfavourable development led to a situation where the bonds between next-nearest neighbouring Ti atoms actually became stronger with increasing AlN fraction. The result is an accelerating driving force for isostructural decomposition in samples with high AlN fraction. In the case of $Cr_{1-x}Al_xN$ it was shown in Ref. 8 that the magnetic split of the Cr d-states placed the Fermi level in the valley between the spin up and spin down bands. This situation changes the effect of the sharpening of the nonbonding states as the Fermi level effectivly moves down the slope of the state, rather than up as in the case of $Ti_{1-x}Al_xN$, leading to a lower mixing enthalpy for $Cr_{1-x}Al_xN$ and a more symmetric shape of the curve.

Fig. 4 shows the DOS of the transition metal atoms, both in the pure MN and in an alloy with a composition of $M_{0.25}Al_{0.75}N$ for all four systems considered here. Although the later composition is unlikely to be possible to realise experimentally, especially for the Ti and Hf containing systems, this high Al content makes any compositional dependent band structure effects more pronounced. The $Ti_{1-x}Al_xN$ system (top left panel) shows the sharpening of de 3d non-bonding state and the disappearance of the low-energy shoulder in the $Ti_{0.25}Al_{0.75}N$ alloy, as was discussed above. In the case of $Cr_{1-x}Al_xN$ (top right panel) the magnetic split of the non-bonding 3d-state is clearly visible with the Fermi level falling in between the peaks. In $Sc_{1-x}Al_xN$ (bottom left panel), having one less valence electron per transition metal compared to $Ti_{1-x}Al_xN$, the non-bonding 3d-state is positioned above the Fermi level already in pure ScN, making the material in our calculation a zero bandgap semiconductor. Since the underestimation of band gaps is a well known issue for GGA (as well as LDA) based calculations, it is not surprising that the experimental bandgap has been measured to 1.3 eV [29]. However, at the high AlN composition the qualitatively same development as in $Ti_{1-x}Al_xN$ can be seen for the non-bonding state but it is now above the Fermi level. The calculated DOS for the $Hf_{1-x}Al_xN$ system is shown in the bottom right panel.

HfN has two distinct differences to the other three systems visible in the DOS. Firstly the extremely sharp and localised 4f-states are visible 12 eV below the Fermi level. However, they are not taking any part in the bonding of the system. Secondly and more relevant, the 5d states are considerably broader compared to the 3d states of the other Ti, Sc and Cr- based systems. However, the same trend, as in the $Ti_{1-x}Al_xN$ system is visible when HfN is mixed with AlN. The low energy shoulder of the non-bonding 5d state dissapears in the DOS of $Hf_{0.25}Al_{0.75}N$ and the Fermi energy is forced up onto a more sharp non-bonding state. It is worth noting that the narrowing of the non-bonding states are counteracted, especially in the case of Sc and Hf, by the broadening that comes with the compression resulting from the decreasing lattice parameters in AlN rich alloys.

Discussion

From this results one can conclude that the narrowing of the non-bonding transition metal d-state is common for all transition metal nitrides considered here, TiN, CrN, ScN and HfN when they are alloyed with AlN. However the valence electron concentration and thus the position of the Fermi level decides whether or not this development affects the mixing enthalpy. In $Sc_{1-x}Al_xN$ this state is above the Fermi level at all AlN fractions and has no impact on the mixing energetics. Instead the high and symmetric mixing enthalpy is a result of the large lattice spacing mismatch between ScN and c-AlN. In $Ti_{1-x}Al_xN$ on the other hand, one electron needs to be accommodated in the non-bonding state. When the hybridisation with the other Ti atoms are diluted as AlN is added, the low energy shoulder of this state gradualy disapears and the Fermi level is forced up onto a sharp atomic-like 3d state of Ti in AlN rich samples. This is increasingly unfavourable and the result is a large and asymmetric contribution to the mixing enthalpy. On the other hand the size mismatch is rather small and can only play a minor role in this system. In $Cr_{1-x}Al_xN$ magnetism is important to understand the bonding physics. CrN has three more valence electrons than ScN. If it had been non-magnetic the Fermi level would have fallen onto the peak of the non-bonding state, capable of accommodating six electrons. However CrN is magnetic and the non-bonding state is split in a spin up and a spin down bands. The spin up states are almost entirely occupied and the Fermi level falls into the valley between the peaks. When the states sharpen as AlN is added the whole spin up non-bonding state falls below the Fermi level and the disappearance of the low energy shoulder is compensated by the corresponding decrease of the high energy shoulder. As a result the band narrowing has no effect on the mixing enthalpy. Since also the lattice mismatch is small between CrN and c-AlN, the mixing enthalpy is rather low. Finally the $Hf_{1-x}Al_xN$ shows clear similarities with the iso-valent $Ti_{1-x}Al_xN$ with a large and asymmetric mixing enthalpy due to the electronic band structure effect. However HfN has also a large lattice mismatch with c-AlN giving a large symmetric contribution the the enthalpy similar to the $Sc_{1-x}Al_xN$ case.

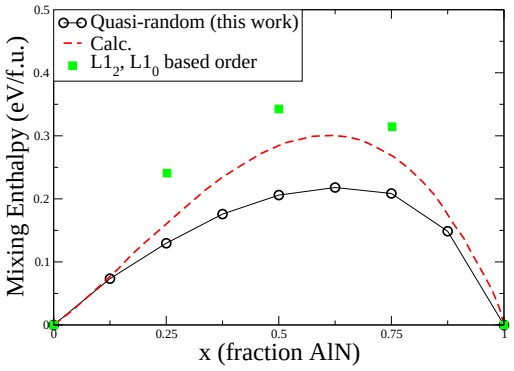

FIG. 1: (Color online) A comparison of the calculated mixing enthalpy of B1 $Ti_{1-x}Al_xN$ in the solid solution phase modelled with the SQS-method (black circles), the values obtained in Ref. [13] (red dashed line) and the ordered $L1_0$ and $L1_2$ based structures (green squares). The SQS method was shown in Ref. [3] to be fully consistent with an analytical CPA treatment of the disorder, proving its reliability.

CONCLUSION

In conclusion we have calculated lattice parameters, electronic density of states and mixing enthalpies of the $Ti_{1-x}Al_xN$, $Cr_{1-x}Al_xN$, $Sc_{1-x}Al_xN$ and $Hf_{1-x}Al_xN$ systems with the transition metal and aluminium forming a solid solution. It was found that in all four systems, the non-bonding transition metal d-state developed into a narrow almost atomic like state as the AlN content increased. However this development effects the mixing enthalpy only in the cases of $Ti_{1-x}Al_xN$ and $Hf_{1-x}Al_xN$ leading to a high and asymmetric mixing enthalpy and an accelarating drivingforce for isostructural decomposition at higher AlN concentrations. A large lattice mismatch adds a symmetric contribution to the mixing enthalpy in the $Sc_{1-x}Al_xN$ and $Hf_{1-x}Al_xN$ systems. A large size mismatch however, allthough adding to the driving force for decomposition, might hinder coherent decomposition and instead promote an incoherent decompositon through nucleation and growth of hexagonal AlN, a process believed to be unfavorable for coating performance.

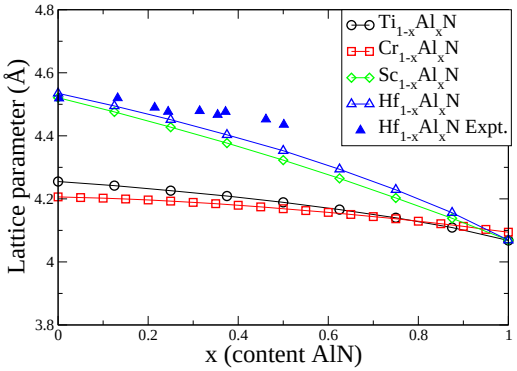

FIG. 2: (Color online) Calculated lattice parameters for B1 $Ti_{1-x}Al_xN$, $Cr_{1-x}Al_xN$, $Sc_{1-x}Al_xN$ and $Hf_{1-x}Al_xN$. The recent experimental values on $Hf_{1-x}Al_xN$ in Ref [9] is shown with filled blue triangles for comparison.

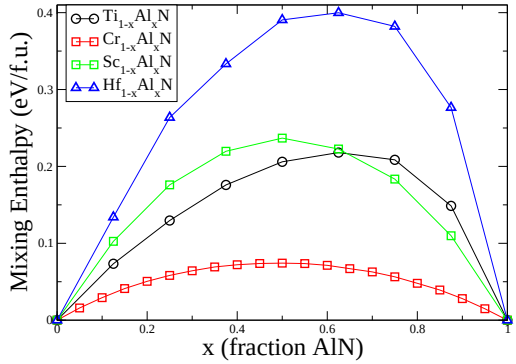

FIG. 3: (Color online) Calculated isostructural mixing enthalpy for B1 $Ti_{1-x}Al_xN$, $Cr_{1-x}Al_xN$, $Sc_{1-x}Al_xN$ and $Hf_{1-x}Al_xN$ with respect to B1 MN and c-AlN in eV/f.u.

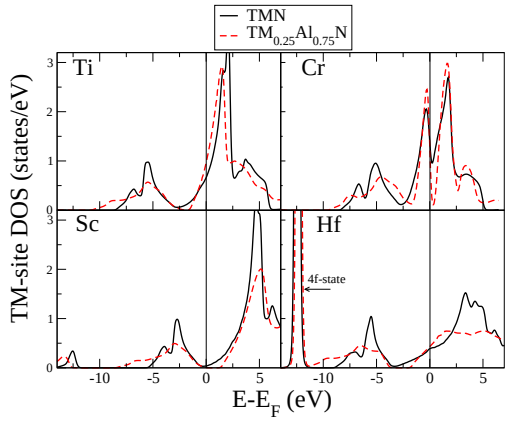

FIG. 4: (Color online) Calculated DOS of the transition metal site for the pure MN as well as in $M_{0.25}Al_{0.75}N$ for the four considered transition metals. Note that the position of the fermilevel decides wheter the sharpening of the non-bonding d-electron state affects the mixing enthalpy or not.

* Electronic address: bjoal@ifm.liu.se

[1] A. Hörling, L. Hultman, M. O. J. Sjölen, and L. Karlsson, Surface and Coatings Technology **191**, 384 (2005).

[2] P. H. Mayrhofer, A. Hörling, L. Karlsson, J. Sjölén, T. Larsson, C. Mitterer, and L. Hultman, Applied Physics Letters **83**, 2049 (2003).

[3] B. Alling, A. V. Ruban, A. Karimi, O. E. Peil, S. I. Simak, L. Hultman, and I. A. Abrikosov, Physical Review B **75**, 045123 (2007).

[4] A. E. Reiter, V. H. Derflinger, B. Hanselmann, T. Bachmann, and B. Sartory, Surface and Coatings Technology **200**, 2114 (2005).

[5] H. Willmann, P. H. Mayrhofer, P. Persson, A. E. Reiter, L. Hultman, and C. Mitterer, Scripta Materiala **54**, 1847 (2006).

[6] R. Sanjinés, O. Banakh, C. Rojas, P. E. Schmid, and F. Lévy, Thin Solid Films **420-421**, 312 (2002).

[7] Y. Makino and K. Nogi, Surf. Coat. Technol. **98**, 1008 (1998).

[8] B. Alling, T. Marten, I. A. Abrikosov, and A. Karimi, Journal of Applied Physics **102**, 044314 (2007).

[9] B. Howe, J. Bareño, M. Sardela, J. G. Wen, J. E. Greene, L. Hultman, A. A. Voevodin, and I. Petrov, Surf. Coat. Technol. **202**, 809 (2007).

[10] C. Höglund, J. Birch, M. Beckers, B. Alling, Z. Czigány, A. Mücklich, and L. Hultman, Eur. J. Inorg. Chem. **In press** (2008).

[11] A. Zunger, S. H. Wei, L. G. Ferreira, and J. E. Bernard, Physical Review Letters **65**, 353 (1990).

[12] J. W. D. Connolly and A. R. Williams, Phys. Rev. B **27**, 5169 (1983).

[13] P. H. Mayrhofer, D. Music, and J. M. Schneider, Applied Physics Letters **88**, 071922 (2006).

[14] P. Soven, Physical Review **156**, 809 (1967).

[15] B. Velický, S. Kirkpatrick, and H. Ehrenreich, Physical Review **175**, 747 (1968).

[16] S. Kirkpatrick, B. Velický, and H. Ehrenreich, Physical Review B **1**, 3250 (1970).

[17] P. E. Blöchl, Physical Review B **50**, 17953 (1994).

[18] G. Kresse and J. Hafner, Physical Review B **48**, 13115 (1993).

[19] G. Kresse and J. Hafner, Physical Review B **49**, 14251 (1994).

[20] H. L. Skriver and N. M. Rosengaard, Physical Review B **43**, 9538 (1991).

[21] I. A. Abrikosov and H. L. Skriver, Physical Review B **47**, 16532 (1993).

[22] A. V. Ruban and H. L. Skriver, Computational Materials Science **15**, 119 (1999).

[23] J. Korringa, Physica **13**, 392 (1947).

[24] W. Kohn and N. Rostoker, Physical Review **94**, 1111 (1954).

[25] O. K. Andersen, Physical Review B **12**, 3060 (1975).

[26] O. K. Andersen and O. Jepsen, Physical Review Letters **53**, 2571 (1984).

[27] J. P. Perdew, K. Burke, and M. Ernzerhof, Physical Review Letters **77**, 3865 (1996).

[28] B. Alling, A. Karimi, L. Hultman, and I. A. Abrikosov, Appl. Phys. Lett. **92**, 071903 (2008).

[29] D. Gall, M. Städele, K. Järrendahl, I. Petrov, P. Desjardins, R. T. Haasch, T. Y. Lee, and J. E. Greene, Phys. Rev. B **63** (2001).